Materials Sciences and Applications, 2023, 14, 458-472
https://www.scirp.org/journal/msa
ISSN Online: 2153-1188
ISSN Print: 2153-117X

Numerical Simulation for Enhancing Performance of MoS_2 Hetero-Junction Solar Cell Employing Cu_2O as Hole Transport Layer

Md. Ferdous Wahid*, Ushna Das, Bidesh Kumer Paul, Shuvo Paul, Md. Nuralam Howlader, Md. Sazedur Rahman

Department of Electrical and Electronic Engineering, Hajee Mohammad Danesh Science and Technology University, Dinajpur, Bangladesh
Email: *mfwahid26@gmail.com

How to cite this paper: Wahid, M.F., Das, U., Paul, B.K., Paul, S., Howlader, M.N. and Rahman, M.S. (2023) Numerical Simulation for Enhancing Performance of MoS_2 Hetero-Junction Solar Cell Employing Cu_2O as Hole Transport Layer. *Materials Sciences and Applications*, **14**, 458-472.
https://doi.org/10.4236/msa.2023.149030

Received: August 5, 2023
Accepted: September 3, 2023
Published: September 6, 2023

Abstract

The paper reported the design and thorough analysis of a thin-film solar cell (TFSC) based on molybdenum disulfide (MoS_2) with an integrated Copper(I) Oxide (Cu_2O) hole transport layer (HTL), employing the one-dimensional Solar Cell Capacitance Simulator (SCAPS-1D) software. By varying crucial parameters such as absorber layer thickness, doping density, and bulk defect density, as well as HTL thickness, doping concentration, and electron affinity, defect density at ZnO/absorber and absorber/Cu_2O interfaces, and operating temperature, we explored key photovoltaic measures including open circuit voltage (Voc), short-circuit current density (Jsc), fill-factor (FF), and power conversion efficiency (PCE) of the hetero-junction solar cell. The study demonstrated an efficiency of 18.87% for the MoS_2 solar cell without HTL, while the proposed solar cell (SC) utilizing Cu_2O HTL and optimized device structure exhibited a remarkable PCE of 26.70%. The outcomes derived from the present study offer valuable insights for the progress of a highly efficient and economically viable MoS_2 hetero-junction TFSC.

Keywords

Solar Cell, Thin Film, SCAPS-1D, Hetero-Junction, HTL, Defect Density

1. Introduction

The rise of the population, urbanization, technological progresses, and the evolving lifestyles are all prophesied to cause a colossal surge in global energy demand in the foreseeable future. Accordingly, it is expected that the energy demand will

reach to 30 terawatts (TW) by 2050 [1]. Currently, a large portion of energy demands are satisfied by the utilization of fossil fuels; nevertheless, this limited resource is approaching a state of exhaustion. Furthermore, the widespread use of fossil fuels is resulting in adverse consequences for the environment, hence necessitating a concerted effort to prioritize the advancement of sustainable and renewable energy alternatives [2]. To mitigate climate change and foster a more environmentally sustainable future for next generations, renewable energy sources including solar, wind, hydropower, biomass, and geothermal needs to be exploited in place of fossil fuels [3]. Solar energy has emerged as a highly promising alternative in the ongoing efforts to mitigate greenhouse gas emissions and address the challenges posed by climate change. It is a plentiful and sustainable form of energy that is harnessed by utilizing SCs to directly convert sunlight into electrical energy [4] [5].

Thin film solar cells have garnered significant attention in the field of photovoltaic technology due to their cost-effectiveness, ease of manufacture and greater efficiency [6]. Amorphous silicon (a-Si), cadmium telluride (CdTe), and copper indium gallium selenide (CIGS) are the three most popular TFSC technologies, with PCE of 9.13%, 20.77%, and 23.03%, respectively [7]. Presently, there is a significant research focus on transition metal dichalcogenide (TMD) materials as promising semiconductors for TFSC. This interest stems from their exceptional energy gap, satisfactory carrier transport properties, and captivating optical absorption characteristics [8] [9]. TMD compounds, specifically MoS_2 have garnered significant attention due to its remarkable light absorption coefficient surpassing 10^5 cm^{-1}, ideal band gap of 1.29 eV, relatively high carrier mobility, eco-friendliness, cost-effectiveness, and abundance in the Earth's crust [10]. The MoS_2-based SC (ITO/MoS_2/Au) exhibited experimental PCE of merely 0.7% with a 110 nm absorber layer thickness and 1.8% with a 220 nm absorber layer thickness [11]. With a PCE of 19.62%, the SC configuration comprising ZnO/CdS/MoS_2 exhibited exceptional performance, thus highlighting the suitability of MoS_2 as a highly effective absorber layer for SCs [12]. The optimized ITO/ZnSe/MoS_2 SC exhibited a theoretical maximum efficiency of 19.48%, while the addition of SnS as HTL to the structure (ITO/ZnSe/MoS_2/SnS), increased the theoretical maximum efficiency to 21.39%. Valance band offset at the HTL/absorber interface significantly improves PCE of SC [13]. Thus, in order to design a highly efficient MoS_2 TFSC, a suitable HTL material with enhanced electrical and optical properties is indispensable. Several inorganic materials, including Cu_2O, CuSCN, CuI, and NiO, have shown promising use as HTL in various organic and inorganic solar cells [14] [15]. Among these options, Cu_2O is a promising material for fulfilling HTL roles due to its indirect bandgap (2.1 - 2.6 eV), electron affinity (3.4 eV), abundance, environmental advantages, and synthesis practicality [16]. The effective extraction of holes is made possible by the synergy between high hole-mobility and precisely matched band alignment with MoS_2.

Therefore, this paper proposed a novel design of a MoS_2-based TFSC em-

ploying Cu_2O as HTL with the structure Al/ZrS_2/ZnO/MoS_2/Cu_2O/Ni. The proposed SC has been designed and examined using SCAPS-1D. The widespread adoption and utilization of SCAPS-1D in the domain of SC numerical simulations can be attributed to its unique combination of open-source nature, versatility, user-friendliness, accuracy, and the active support from its community of users and developers [1] [6] [10]. The numerical calculations revealed that this new design resulted in a substantial improvement in SC performance. This study explores the utilization of Cu_2O as HTL to enhance device performance, reaching a maximum efficiency of 26.70% with Voc is 1.089 V, Jsc is 30.33 mA/cm^2, FF is 80.85% whereas without HTL the maximum efficiency of 18.87% with Voc is 0.9425 V, Jsc is 25.41 mA/cm^2, FF is 78.79%. Additionally, we delve into the impacts of altering the thickness of the absorber layer and HTL, alongside varying the doping concentration and defect density of the absorber layer, the doping concentration and electron affinity of HTL, interface defect density, and temperature. The ultimate goal is to attain enhanced efficiency through careful examination of these factors.

2. Device Architecture and Material Parameters

The SCAPS-1D, Version 3.9 software was utilized for the design and performance analysis of the proposed Al/ZrS_2/ZnO/MoS_2/Cu_2O/Ni SC configuration. The Department of Electronics and Information Systems at the University of Ghent, Belgium, has developed a sophisticated software that meticulously analyzes the electrostatic potential and behavior of free carriers within the solar cell. This software achieves its insights by skillfully incorporating continuity equations and the Poisson equation [17]. **Figure 1(a)** illustrates the schematic diagram of the hetero-junction structure used in the simulation. The SC comprises a p-MoS_2 absorber layer, an n-ZrS_2 (Zirconium disulfide) window layer, an n-ZnO electron transport layer (ETL), and a Cu_2O HTL. In this design, Al is utilized as the front contact material, while Ni functions as the back contact material, forming a well-structured device for efficient solar energy conversion. ZrS_2 used as window layer, a type of TMDCs, is one of the most promising photovoltaic materials due to its high absorption coefficient and variable bandgap energy of 1.2 - 2.2 eV, allowing for successful energy conversion and device engineering [18]. ZnO is used as ETL because to its cost-effectiveness, physical and chemical stability, and non-toxicity. The wide bandgap of ZrS_2 (2.0 eV) and ZnO (3.27 eV) play a crucial role in the hetero-junction structure by allowing significant optical throughput. Additionally, the desirable electron affinity of the ZnO (~4.1 eV) ETL enables it to form a suitable junction with MoS_2 absorber layer. Furthermore, Cu_2O is used as HTL, effectively reducing the recombination loss of photo-generated carriers at the back edge [19] [20]. **Figure 1(b)** shows the energy band diagram of the reported SC structure. All simulations are conducted at a working temperature of 300 K, with AM 1.5 G light. Leveraging prior research findings, we have integrated experimentally and theoretically derived

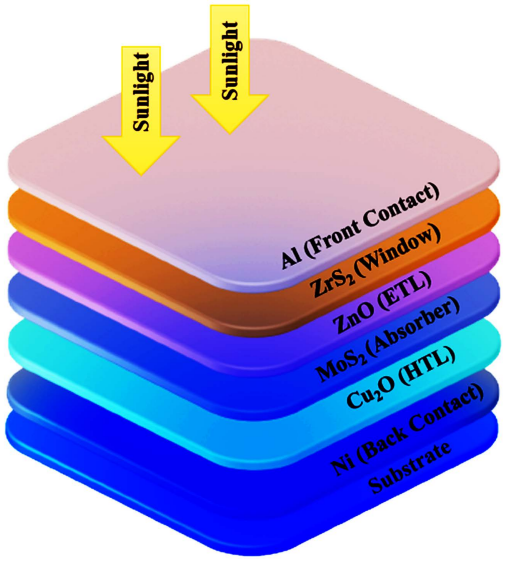

(a)

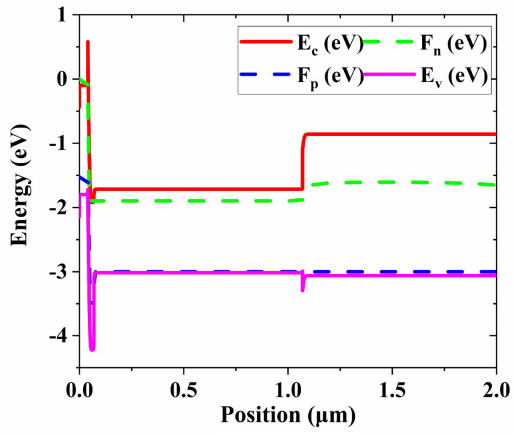

(b)

Figure 1. The schematic (a) proposed Al/ZrS_2/ZnO/MoS_2/Cu_2O/Ni structure (b) Energy band.

parameters of different layers to optimize the performance of the recently developed MoS_2 SC with Cu_2O HTL. The pertinent physical parameters for each layer have been delineated in Table 1 and Table 2.

3. Result and Discussion

3.1. Influence of Absorber Layer Thickness and Doping Concentration on PV Parameters

Figure 2 demonstrated a comprehensive analysis of photovoltaic (PV) parameters for MoS_2-based hetero-junction TFSC, considering variations in MoS_2 thickness and acceptor concentration. It is evident from Figure 2(a) that the Voc exhibits minor fluctuations in response to changes in thickness. Moreover, a notable increase in Voc is observed when the acceptor concentration is raised from 10^{17} to 10^{21} cm^{-3}, resulting in a rise from 0.96 V to 1.20 V [13].

Table 1. Material parameters employed in our simulations [2] [10] [18].

Parameters	ZrS_2	ZnO	MoS_2	Cu_2O
Thickness (μm)	0.04	0.03	1	0.04
Band gap, Eg (eV)	1.7	2.3	1.3	2.2
Electron affinity, χ (eV)	4.7	4	4	3.4
Permittivity(Relative), εr	16.4	9	13.60	7.5
CB density of states, N_C (1/cm^3)	2.2×10^{19}	3.7×10^{18}	2.2×10^{18}	2×10^{19}
VB density of states, N_V (1/cm^3)	1.8×10^{19}	1.8×10^{19}	1.8×10^{19}	1.0×10^{19}
Mobility(Electron), μ_n (cm^2/Vs)	300	100	100	200
Mobility(Hole), μ_h (cm^2/Vs)	30	25	25	8600
Acceptor density, N_A (1/cm^3)	0	0	1×10^{19}	1×10^{18}
Donor density, N_D (1/cm^3)	1×10^{21}	1×10^{19}	0	0
Defect type	Neutral	Single-Acceptor	Single-Donor	Neutral
Energy distribution	Single	Gaussian	Gaussian	Single
Defect density, Nt (1/cm^3)	1×10^{15}	1×10^{14}	1×10^{14}	1×10^{14}

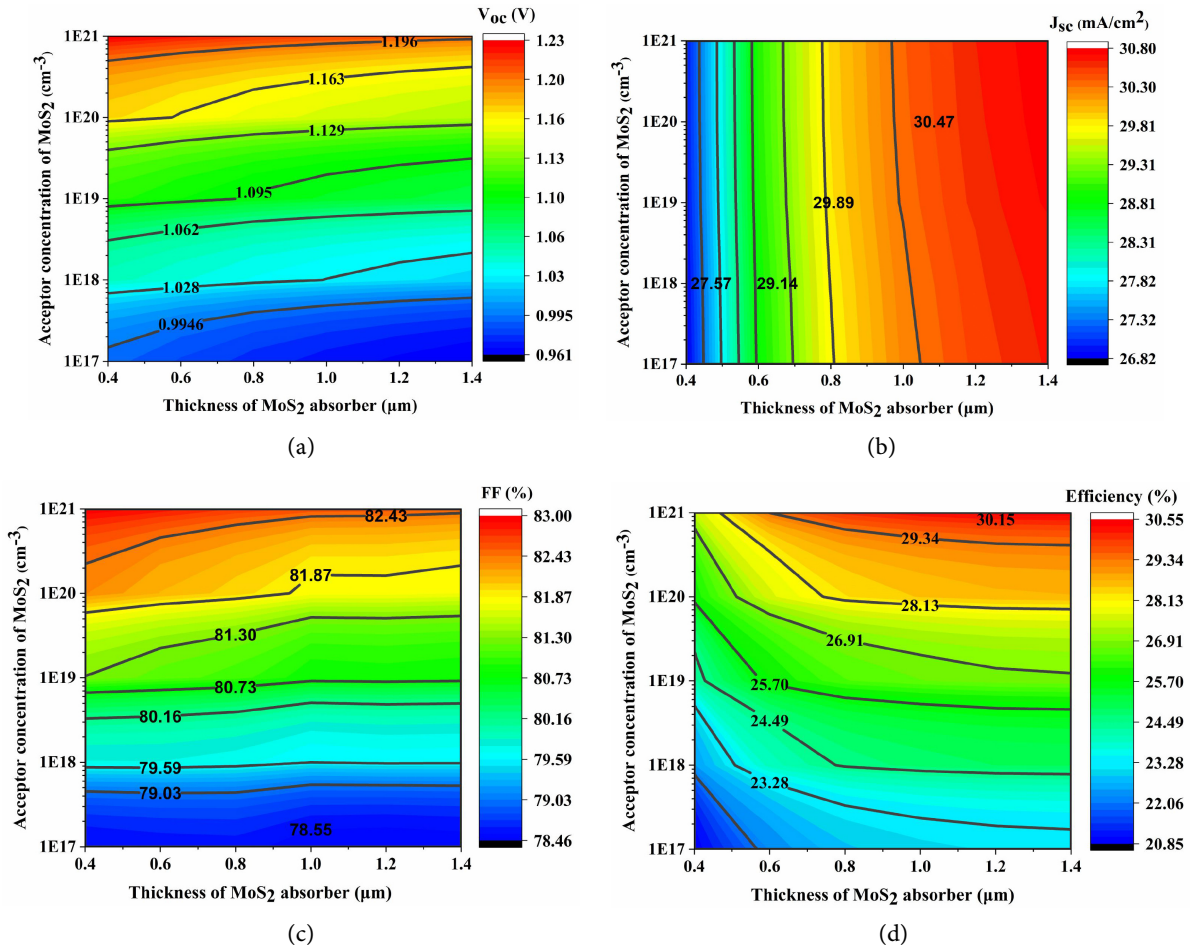

Figure 2. (a) Voc, (b) Jsc, (c) FF and (d) efficiency as function on the absorber (MoS_2) layer thickness and the acceptor concentration.

Table 2. Input parameters of interface defect layers [10] [18].

Interface	Defect type	Capture cross section: Electrons/holes(cm^2)	Energetic distribution	Reference for defect energy level	Total density (cm^{-3})
ZrS_2/ZnO	Neutral	1×10^{-19} 1×10^{-19}	Single	Above the highest EB	1×10^{10}
ZnO/MoS_2	Neutral	1×10^{-19} 1×10^{-19}	Single	Above the highest EB	1×10^{10}
MoS_2/Cu_2O	Neutral	1×10^{-18} 1×10^{-18}	Single	Above the highest EB	1×10^{10}

Figure 2(b) shows that Jsc increases with thickness and acceptor concentration. However, it is noteworthy that the impact of MoS_2 thickness on Jsc is significantly greater, since the increase in thickness is directly related to increased light absorption, which subsequently results in a higher creation of hole-electron pairs. As the acceptor concentration increases, the FF demonstrates an upward trend, whereas the impact of MoS_2 thickness on FF is found to be minimal when the acceptor concentration increases, as depicted in Figure 2(c). Finally, the efficiency of the SC exhibits an increase from 20.85% to 24.49% as the thickness of MoS_2 is elevated from 0.4 μm to 1 μm, alongside an increase in the acceptor concentration from 10^{17} to 10^{21} cm^{-3}, as illustrated in Figure 2(d). For the simulation, a thickness of 1 μm for MoS_2 absorber layer and an acceptor concentration of 10^{19} cm^{-3} were identified as the optimal values.

3.2. Impact on PV Parameters Due to Defects in MoS_2 Absorber Layer

Figure 3 depicted the dependence of PV performance parameters on absorber defect density, which ranges from 10^{12} to 10^{16} cm^{-3}. At a defect density 10^{12} cm^{-3} the maximum values of Voc Jsc, FF, and efficiency are obtained. As a consequence of Shockley-Read Hall non-radiative recombination, there is a decrease in the minority charge carrier lifetime and an increase in recombination carriers within the absorber layer, leading to a reduction in Voc, FF, and PCE with higher defect density [21] [22] [23]. Nonetheless, it is observed that the Jsc remains relatively stable until the defect density reaches 10^{15} cm^{-3}. Beyond this point, Jsc begins to decrease, likely attributed to heightened carrier recombination, which reduces the number of available carriers responsible for generating the short-circuit current. Consequently, the optimal value for the defect density of MoS_2 is 10^{14} cm^{-3}.

3.3. Effect of HTL Thickness, Doping Density and Electron Affinity on PV Parameters

Figure 4 illustrated the impact of Cu_2O thickness, doping density, and electron affinity on PV parameters. As depicted in Figure 4(a) and Figure 4(b), the variations in Cu_2O thickness and doping density do not exhibit a significant effect

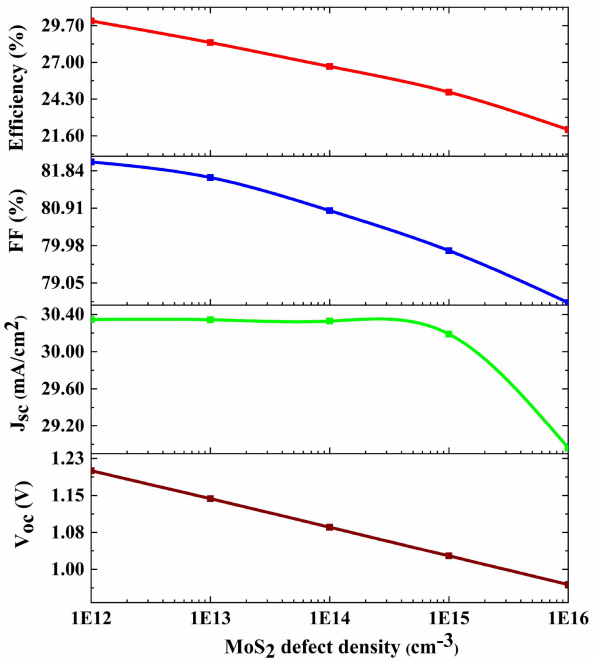

Figure 3. Performance parameters as a function of defect density in MoS_2 absorber layer.

on the PV parameters. However, the electron affinity of Cu_2O exerts a substantial influence on enhancing the PV parameters [24]. Notably, as the electron affinity increases up to 3.4 eV, all PV parameters exhibit a consistent upward trend, as illustrated in **Figure 4(c)**. The investigation yields the determination of the optimal values for the thickness of the HTL and the doping density, which are found to be 0.4 μm and 10^{16} cm^{-3}, respectively. Additionally, the electron affinity of the HTL is found to be 3.4 eV, indicating a favorable characteristic for the overall performance of the device.

3.4. Influence of Interfacial Defect Density on PV Parameters

Figure 5(a) and **Figure 5(b)** provide a depiction of the influence of interfacial defect density variations, spanning from 10^{10} cm^{-2} to 10^{18} cm^{-2}, at the ZnO/MoS_2 and MoS_2/Cu_2O interfaces on PV parameters. As the defect density approaches 10^{18} cm^{-2}, there is a notable and significant decrease observed in all PV parameters. The presence of trap states at the interface acts as recombination centers, resulting in a reduction in photo-generated carriers and hindering efficient carrier collection. These defects related to interface states significantly diminish the overall performance parameters [1]. The value of 10^{11} cm^{-2} for interfacial defect density has been specified for both interfaces in order to reach a balance on PV characteristics.

3.5. Impact of Temperature on PV Parameters

The assessment of PV parameters, namely Voc, Jsc, PCE, and FF, has been conducted to investigate the impact of temperature fluctuations ranging from 275 K to 475 K, as depicted in **Figure 6**. It has been apparent that enhancing the oper-

ating temperature results in a reduction of the Voc. As temperature increases, the band gap of MoS_2 decreases and the reverse saturation current is enhanced, both of which lead to a decline in Voc [25]. Conversely, the values of Jsc exhibit a slight increase with elevating operating temperatures, owing to the increase in generation of electron-hole pairs [26] [27]. The proposed SC has an estimated FF of 80.18% at 275 K and 85.48% at 360 K, after which it declines to 81.84% as the temperature goes up. It is also noticed from **Figure 6** that PCE of the proposed SC exhibits lower value at high temperature as a consequence of reduced Voc.

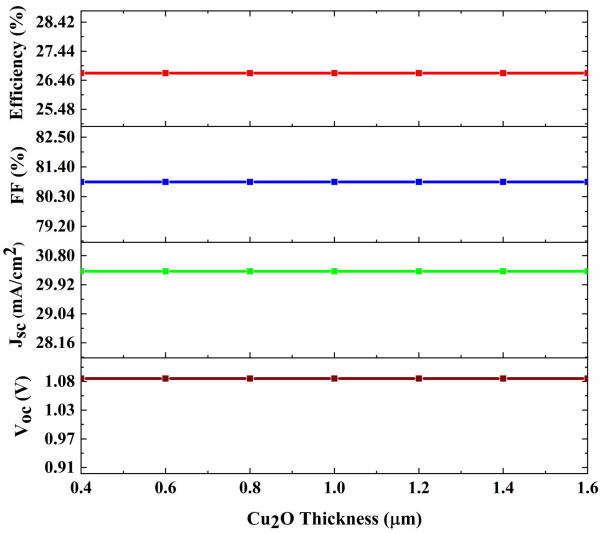

(a)

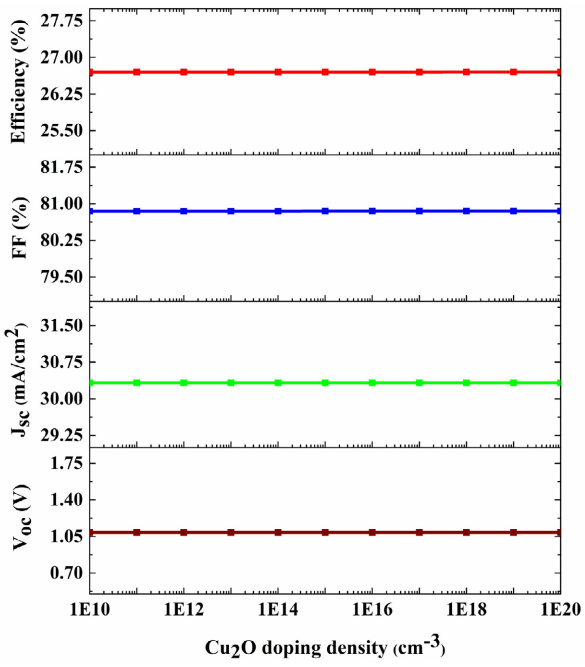

(b)

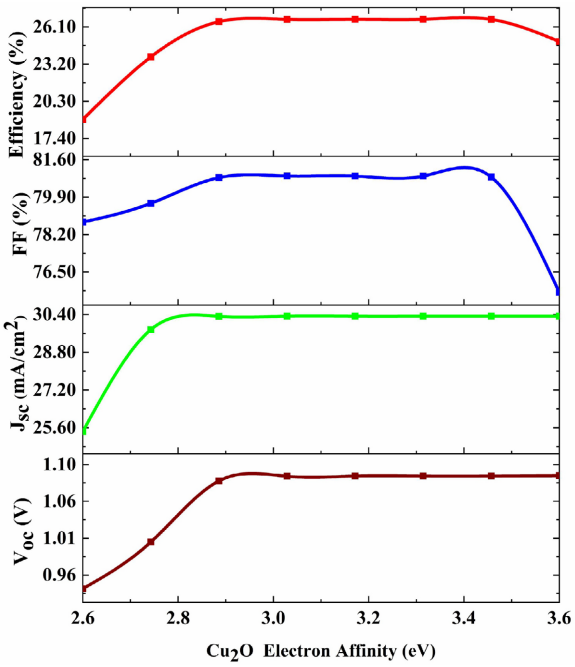

(c)

Figure 4. The effect of HTL layer (a) thickness (b) doping density (c) electron affinity on PV parameters.

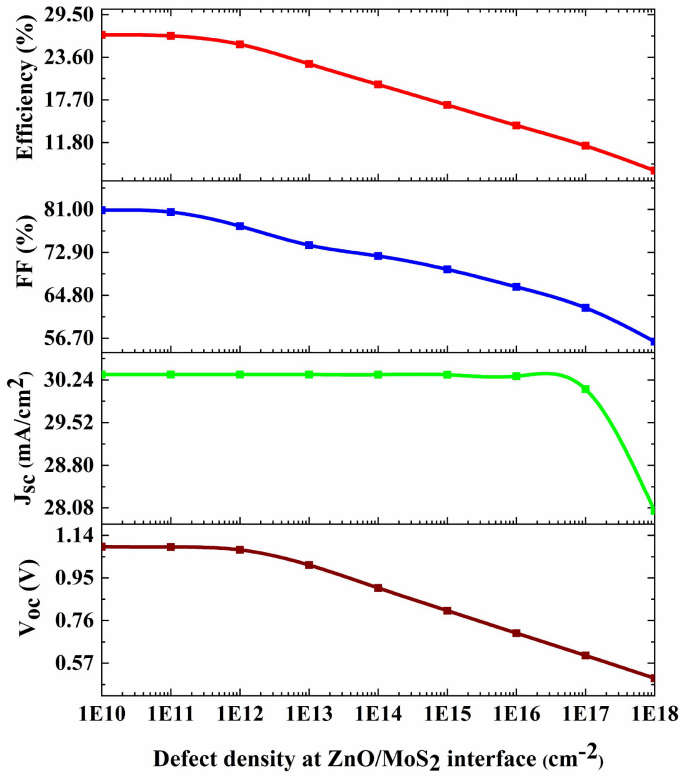

(a)

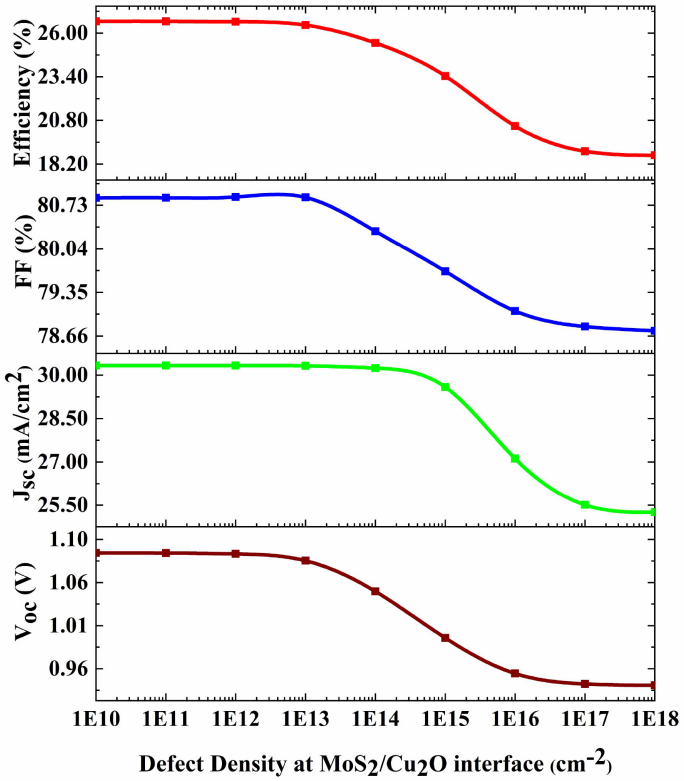

(b)

Figure 5. The change of output parameters due to the variation of defect density at (a) ZnO/MoS_2 and (b) MoS_2/Cu_2O interface.

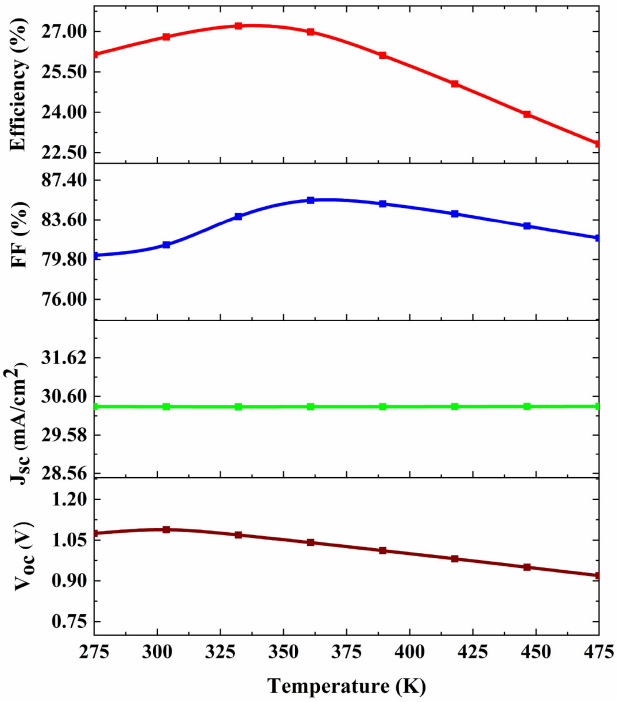

Figure 6. The impact of temperature on PV parameters.

3.6. Influence of HTL on SC Output Characteristics

Figure 7(a) and **Figure 7(b)** present the J-V characteristics and Quantum Efficiency (QE) curves for the optimized designed MoS_2-based TFSC with and without HTL layer. Through numerical simulation, the values of Voc, Jsc, FF, and PCE for the newly designed Al/ZrS_2/ZnO/MoS_2/Cu_2O/Ni hetero-junction SC were estimated to be 1.089 V, 30.33 mA/cm^2, 80.85%, and 26.70%, respectively. In comparison, the Al/ZrS_2/ZnO/MoS_2/Ni SC exhibited Voc, Jsc, FF, and PCE values of 0.9425 V, 25.41 mA/cm^2, 78.79%, and 18.87%, respectively. Notably, the presence of Cu_2O in the structure significantly increases the calculated SC parameters compared to the structure without Cu_2O. The improvement of Voc, Jsc, FF and PCE is due to reduction of dark current for surface recombination [28] [29] [30]. The MoS_2-based TFSC without HTL suffers from a high rate of minority carrier recombination, leading to reduced performance parameters, especially a lower Voc value. In contrast to the structure without HTL, as shown in **Figure 7(b)**, the QE with the Cu_2O HTL layer is higher.

3.7. Comparative Study

Table 3 presents a comprehensive analysis of MoS_2-based TFSC architectures that have been examined in previous research studies. The numerical simulations of the MoS_2-based TFSC with Cu_2O HTL demonstrated superior solar cell performance compared to previous studies. In this study, the advantage of incorporating Cu_2O HTL with MoS_2-based TFSCs has been investigated. Cu_2O and MoS_2 exhibit better energy level alignment which is essential for enhancing the performance of PV parameters.

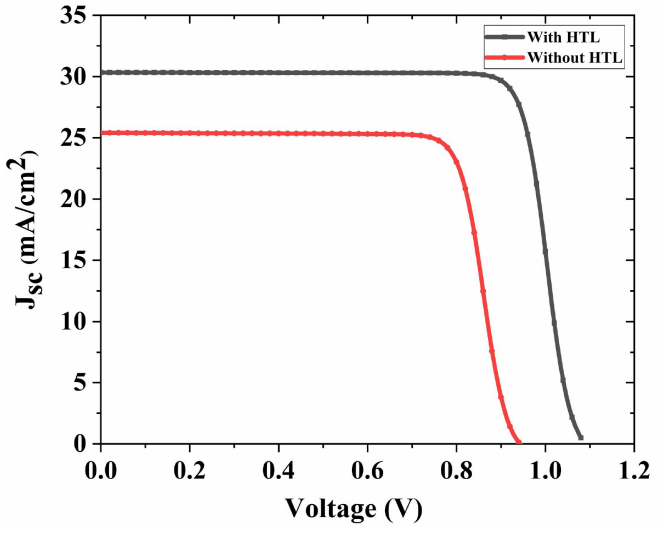

(a)

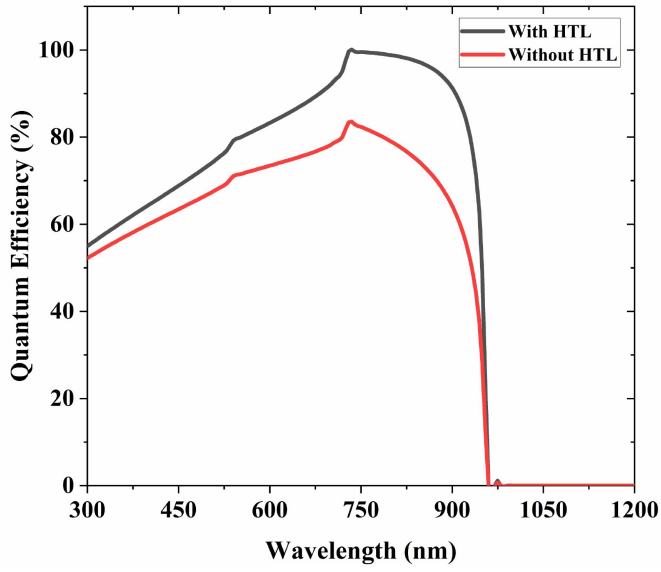

(b)

Figure 7. The numerically examined (a) JV curves with HTL and without HTL; (b) QE curve with HTL and without HTL of the Proposed SC.

Table 3. Comparison of proposed optimized SC with the previously reported studies.

Device Structure	Voc (V)	Jsc (mA/cm^2)	FF (%)	Efficiency (%)	Ref.
Al/ITO/TiO_2/MoS_2/Ni	0.793	30.89	80.62	22.30	[1]
Al/FTO/CdS/MoS_2/Ni	0.76	34.11	82.80	21.61	[10]
FTO/ZnO/MoS_2/Cu_2O/Au	0.93	36.65	76.88	19.62	[12]
CdS/ZnO/MoS_2/Mo	1.014	24.47	85.30	21.17	[31]
ITO/TiO_2/CdS/MoS_2/C/Ag	0.87	15.52	74.48	10.77	[32]
ZrS_2/ZnO/MoS_2/Cu_2O	1.09	30.32	80.85	26.70	This work

4. Conclusion

In this paper, we have presented an investigation of the MoS_2-based TFSC structure Al/ZrS_2/ZnO/MoS_2/Cu_2O/Ni. By employing the SCAPS-1D software and conducting numerical calculations, the study demonstrates a significant enhancement in MoS_2-based TFSC performance with Cu_2O HTL, as compared to MoS_2-based TFSC without Cu_2O HTL. This study explores the utilization of Cu_2O HTL, which has demonstrated notable advancements in key SC parameters, reaching a maximum efficiency of 26.70% with Voc of 1.089 V, Jsc of 30.33 mA/cm^2 and FF of 80.85%. HTL foster the effective charge extraction, collection and transport, while also aiding in minimizing charge recombination which in turns significantly enhanced the SC performance. The optimal thickness of the MoS_2 absorber is 1 μm with acceptor concentration of 10^{19} cm^{-3} and defect density 10^{14} cm^{-3}. Furthermore, the MoS_2/ZnO and Cu_2O/MoS_2 interface defects were estimated to be 10^{11} cm^{-3}. In future, density functional theory can be used to explain the optoelectronic properties of MoS_2 absorber.

Acknowledgements

The University of Gent's Prof. Marc Burgelman and his colleagues kindly provided the SCAPS-1D software that is discussed in this article, and the authors are appreciative of their assistance.

Conflicts of Interest

The authors declare no conflicts of interest regarding the publication of this paper.

References

[1] Ali, M.H., Al Mamun, M.A., Haque, M.D., Rahman, M.F., Hossain, M.K. and Touhidul Islam, A.Z.M. (2023) Performance Enhancement of an MoS_2-Based Heterojunction Solar Cell with an In_2Te_3 Back Surface Field: A Numerical Simulation Approach. *ACS Omega*, **8**, 7017-7029. https://doi.org/10.1021/acsomega.2c07846

[2] Patel, P.K. (2021) Device Simulation of Highly Efficient Eco-Friendly $CH_3NH_3SnI_3$ Perovskite Solar Cell. *Scientific Reports*, **11**, Article No. 3082. https://doi.org/10.1038/s41598-021-82817-w

[3] Nsafon, B.E.K., Owolabi, A.B., Butu, H.M., Roh, J.W., Suh, D. and Huh, J.S. (2020) Optimization and Sustainability Analysis of PV/Wind/Diesel Hybrid Energy System for Decentralized Energy Generation. *Energy Strategy Reviews*, **32**, Article ID: 100570. https://doi.org/10.1016/j.esr.2020.100570

[4] Naveen, S., Aravind, S., Yamini, B., Vasudhareni, R., Gopinath, K.P., Arun, J. and Pugazhendhi, A. (2023) A Review on Solar Energy Intensified Biomass Valorization and Value-Added Products Production: Practicability, Challenges, Techno Economic and Lifecycle Assessment. *Journal of Cleaner Production*, **405**, Article ID: 137028. https://doi.org/10.1016/j.jclepro.2023.137028

[5] Paraschiv, L.S. and Paraschiv, S. (2023) Contribution of Renewable Energy (Hydro, Wind, Solar and Biomass) to Decarbonization and Transformation of the Electricity Generation Sector for Sustainable Development. *Energy Reports*, **9**, 535-544.

https://doi.org/10.1016/j.egyr.2023.07.024

[6] Jha, V., Dasgupta, S. and Ganguly, A. (2023) Study of PbS Nanomaterial Sensitized ZnO Based Solar Cell Using SCAPS-1D Simulator. *2023 International Symposium on Devices, Circuits and Systems* (*ISDCS*), Higashihiroshima, 29-31 May 2023, 1-3. https://doi.org/10.1109/ISDCS58735.2023.10153556

[7] Moon, M.M.A., Rahman, M.F., Hossain, J. and Ismail, A.B.M. (2019) Comparative Study of the Second Generation a-Si:H, CdTe, and CIGS Thin-Film Solar Cells. *Advanced Materials Research*, **1154**, 102-111. https://doi.org/10.4028/www.scientific.net/AMR.1154.102

[8] Zaidi, B., Shekhar, C., Hadjoudja, B., Gagui, S. and Chouial, B. (2019) Optimization of Highly Efficient Monolayer $MoSe_2$ Based Solar Cells. *Acta Physica Polonica A*, **136**, 495-497. https://doi.org/10.12693/APhysPolA.136.495

[9] Zaidi, B., Shekhar, C., Hadjoudja, B., Gagui, S. and Saeed, M.A. (2021) Efficiency Enhancement of Transition Metal Dichalcogenide Based Solar Cells. *Transactions on Electrical and Electronic Materials*, **22**, 687-690. https://doi.org/10.1007/s42341-021-00284-6

[10] Haque, M.D., Ali, M.H., Rahman, M.F. and Islam, A.Z.M.T. (2022) Numerical Analysis for the Efficiency Enhancement of MoS_2 Solar Cell: A Simulation Approach by SCAPS-1D. *Optical Materials*, **131**, Article ID: 112678. https://doi.org/10.1016/j.optmat.2022.112678

[11] Tsai, M.L., Su, S.H., Chang, J.K., Tsai, D.S., Chen, C.H., Wu, C.I., Li, L.J., Chen, L.J. and He, J.H. (2014) Monolayer MoS_2 Heterojunction Solar Cells. *ACS Nano*, **8**, 8317-8322. https://doi.org/10.1021/nn502776h

[12] Rashid, H., Rahman, K.S., Hossain, M.I., Tabet, N., Alharbi, F.H. and Amin, N. (2014) Prospects of Molybdenum Disulfide (MoS_2) as an Alternative Absorber Layer Material in Thin Film Solar Cells from Numerical Modeling. *Chalcogenide Letter*, **11**, 397-403.

[13] Dey, M., Shahriar, M.F., Ali, A., Dey, M. and Das, N.K. (2019) Design and Optimization of an Efficient Molybdenum Disulfide (MoS_2) Solar Cell with Tin Sulfide BSF. *2019 International Conference on Electrical, Computer and Communication Engineering* (*ECCE*), Cox'sBazar, 7-9 February 2019, 1-5. https://doi.org/10.1109/ECACE.2019.8679178

[14] Casas, G., Cappelletti, M., Cédola, A., Soucase, B.M. and Peltzer y Blancá, E. (2017) Analysis of the Power Conversion Efficiency of Perovskite Solar Cells with Different Materials as Hole-Transport Layer by Numerical Simulations. *Superlattices and Microstructures*, **107**, 136-143. https://doi.org/10.1016/j.spmi.2017.04.007

[15] Li, S., Cao, Y.L., Li, W.H. and Bo, Z.S. (2021) A Brief Review of Hole Transporting Materials Commonly Used in Perovskite Solar Cells. *Rare Metals*, **40**, 2712-2729. https://doi.org/10.1007/s12598-020-01691-z

[16] Markose, K.K., Shaji, M., Bhatia, S., Nair, P.R., Saji, K.J., Antony, A. and Jayaraj, M.K. (2020) Novel Boron-Doped p-Type Cu_2O Thin Films as a Hole-Selective Contact in c-Si Solar Cells. *ACS Applied Materials & Interfaces*, **12**, 12972-12981. https://doi.org/10.1021/acsami.9b22581

[17] Burgelman, M. and Marlein, J. (2008) Analysis of Graded Band Gap Solar Cells with SCAPS. 23*rd European Photovoltaic Solar Energy Conference*, Valencia, 1-5 September 2008, 2151-2155.

[18] Abdelfatah, M., El Sayed, A.M., Ismail, W., Ulrich, S., Sittinger, V. and El-Shaer, A. (2023) SCAPS Simulation of Novel Inorganic ZrS_2/CuO Heterojunction Solar Cells. *Scientific Reports*, **13**, Article No. 4553. https://doi.org/10.1038/s41598-023-31553-4

[19] Shah, D.K., KC, D., Muddassir, M., Akhtar, M.S., Kim, C.Y. and Yang, O.B. (2021) A Simulation Approach for Investigating the Performances of Cadmium Telluride Solar Cells Using Doping Concentrations, Carrier Lifetimes, Thickness of Layers, and Band Gaps. *Solar Energy*, **216**, 259-265. https://doi.org/10.1016/j.solener.2020.12.070

[20] Doroody, C., Rahman, K.S., Rosly, H.N., Harif, M.N., Haque, F., Tiong, S.K. and Amin, N. (2020) Impact of High Resistivity Transparent (HRT) Layer in Cadmium Telluride Solar Cells from Numerical Simulation. *Journal of Renewable and Sustainable Energy*, **12**, Article ID: 023702. https://doi.org/10.1063/1.5132838

[21] Devi, N., Parrey, K.A., Aziz, A. and Datta, S. (2018) Numerical Simulations of Perovskite Thin-Film Solar Cells Using a CdS Hole Blocking Layer. *Journal of Vacuum Science & Technology B, Nanotechnology and Microelectronics: Materials, Processing, Measurement, and Phenomena*, **36**, Article ID: 04G105. https://doi.org/10.1116/1.5026163

[22] Nalianya, M.A., Awino, C., Barasa, H., Odari, V., Gaitho, F., Omogo, B. and Mageto, M. (2021) Numerical Study of Lead Free $CsSn_{0.5}Ge_{0.5}I_3$ Perovskite Solar Cell by SCAPS-1D. *Optik*, **248**, Article ID: 168060. https://doi.org/10.1016/j.ijleo.2021.168060

[23] Et-taya, L., Ouslimane, T. and Benami, A. (2020) Numerical Analysis of Earth-Abundant $Cu_2ZnSn(S_xSe_{1-x})_4$ Solar Cells Based on Spectroscopic Ellipsometry Results by Using SCAPS-1D. *Solar Energy*, **201**, 827-835. https://doi.org/10.1016/j.solener.2020.03.070

[24] Kale, A.J., Chaurasiya, R. and Dixit, A. (2021) Inorganic Lead-Free $Cs_2AuBiCl_6$ Perovskite Absorber and Cu_2O Hole Transport Material Based Single-Junction Solar Cells with 22.18% Power Conversion Efficiency. *Advanced Theory and Simulations*, **4**, Article ID: 2000224. https://doi.org/10.1002/adts.202000224

[25] Khatun, M.M., Sunny, A. and Al Ahmed, S.R. (2021) Numerical Investigation on Performance Improvement of WS_2 Thin-Film Solar Cell with Copper Iodide as Hole Transport Layer. *Solar Energy*, **224**, 956-965. https://doi.org/10.1016/j.solener.2021.06.062

[26] Chen, A. and Zhu, K. (2012) Computer Simulation of a-Si/c-Si Heterojunction Solar Cell with High Conversion Efficiency. *Solar Energy*, **86**, 393-397. https://doi.org/10.1016/j.solener.2011.10.015

[27] Abdalmageed, H.I., Fedawy, M. and Aly, M.H. (2021) Effect of Absorber Layer Bandgap of CIGS-Based Solar Cell with (CdS/ZnS) Buffer Layer. *Journal of Physics: Conference Series*, **2128**, Article ID: 012009. https://doi.org/10.1088/1742-6596/2128/1/012009

[28] Taguchi, M., Terakawa, A., Maruyama, E. and Tanaka, M. (2005) Obtaining a Higher V_{oc} in HIT Cells. *Progress in Photovoltaics: Research and Applications*, **13**, 481-488. https://doi.org/10.1002/pip.646

[29] Glunz, S.W., Biro, D., Rein, S. and Warta, W. (1999) Field-Effect Passivation of the SiO_2Si Interface. *Journal of Applied Physics*, **86**, 683-691. https://doi.org/10.1063/1.370784

[30] Atowar Rahman, M. (2021) Enhancing the Photovoltaic Performance of Cd-Free Cu_2ZnSnS_4 Heterojunction Solar Cells Using SnS HTL and TiO_2 ETL. *Solar Energy*, **215**, 64-76. https://doi.org/10.1016/j.solener.2020.12.020

[31] Hossain, M.I., Alharbi, F.H., El-Mellouhi, F. and Tabet, N. (2018) Design Optimization of Solar Cell with Molybdenum Sulfide as Light Absorber. *Journal of Photonics for Energy*, **8**, Article ID: 025501. https://doi.org/10.1117/1.JPE.8.025501

[32] Wu, F., Li, H., Yao, L., Lin, W., Lin, L., Chen, W., Wei, D., Liu, S., Chen, S. and Chen, G. (2021) *In-situ* Hydrothermal Growth of MoS_2 Absorber Layer for Planar Heterojunction Solar Cells. *Solar Energy*, **230**, 754-763. https://doi.org/10.1016/j.solener.2021.10.064